

# Photon ring bounds of scalar hairy charged black holes

Yun Soo Myung\*

Institute of Basic Sciences and Department of Computer Simulation, Inje University,  
Gimhae 50834, Korea

## Abstract

We study photon rings of constant scalar hairy black holes with mass  $m$ , charge  $Q$ , and scalar hair  $S$  obtained from the Einstein-Maxwell-conformally coupled scalar theory. These black holes are classified as scalar hairy Reissner-Nordström black hole, scalar hairy charged black hole with  $S \geq -Q^2$ , and mutated-RN black hole (Einstein-Rosen bridge). The first two respect both dominant and strong energy conditions and have positive effective Newton constant, while the last does not respect two energy conditions and has negative effective Newton constant. These black holes could be candidates for testing whether they satisfy the lower bound of photon ring of  $r_\gamma \geq 1.2r_+$  proposed recently. We obtain all real bounds of photon rings for these black holes and discuss physical and observational properties of real bounds.

Typeset Using L<sup>A</sup>T<sub>E</sub>X

---

\*e-mail address: ysmyoung@inje.ac.kr

# 1 Introduction

No-hair theorem states that an asymptotically flat black hole is completely described by mass  $M$ , electric charge  $Q$ , and angular momentum  $J$  [1]. In this direction, a minimally coupled scalar does not obey the Gauss-law and thus, a black hole is unlikely to have any scalar hairs [2]. On the other hand, introducing the Einstein-conformally coupled scalar theory, one has found the BBMB black hole with mass  $m$  and scalar hair  $\phi(r)$  which blows up on the horizon [3, 4]. This is the first counterexample to the no-hair theorem. However, thermodynamical properties of the BBMB black hole are not promising because the Hawking temperature is always zero and its entropy becomes infinite [5, 6]. Also, it turned out that the BBMB black hole is unstable against perturbations [7]. Its series (numerical) solution was found in [8]. For the BBMB black hole, the photon ring (null unstable circular geodesics) is located at  $r_\gamma = 2m$  where the effective Newton constant diverges [9]. The uniqueness of the outside region of the photon ring has been proved [10, 11].

It is well known that closed photon rings are of importance in determining the physical and observational properties of black hole spacetimes [12, 13, 14]. Very recently, it was shown that the lower bound on the photon ring radius  $r_\gamma$  of black holes is determined by  $r_\gamma \geq 1.2r_+$  if one chooses Einstein gravity with a traceless energy-momentum tensor  $T^\mu{}_\nu = \text{diag}[-\rho, p, p_T, p_T]$  and  $\rho = p + 2p_T$  [15]. Two examples to be tested are recommended as Reissner-Nordström (RN) and Einstein-Yang-Mills black holes. In the case of RN black hole, its real bound is given by  $1.5 \leq r_\gamma/r_+ \leq 2$ . Therefore, the RN black hole respects the lower bound ( $r_\gamma \geq 1.2r_+$ ). However, it is not easy to test Einstein-Yang-Mills black holes because their solutions were known numerically [16, 17, 18, 19, 20].

Photon rings of constant scalar hairy charged black holes [21] were extensively used to describe the shadow of M87\* supermassive black hole [22] and gravitational lensing effects of M87\* and SgrA\* supermassive black holes [23]. It is important to note that these black holes are found from the Einstein-Maxwell-conformally coupled scalar theory whose stress-energy tensor is traceless on-shell configuration. The introduction of the Maxwell term admits a regular (constant) scalar field on and outside the event horizon. So, these constant scalar hairy black holes could be another candidate for testing the photon ring bounds.

In this work, we wish to employ constant scalar hairy charged black holes with mass  $m$ , charge  $Q$ , and scalar hair (charge)  $S$  to derive the real bounds for the ratio of photon

ring radius to horizon radius. According to photon ring bounds, these black holes with mass  $m = 1$  are classified into scalar hairy RN (SHRN) black holes with  $0 < S < 1$  and  $0 < Q < \sqrt{1 - S}$ , scalar hairy charged black hole with  $-Q^2 < S < 0$ , and mutated-RN black hole (Einstein-Rosen bridge) with  $S < -Q^2$  [24]. We obtain all real bounds of photon rings for these black holes and discuss physical and observational properties of real bounds. Furthermore, we will derive the ratio of photon ring to horizon for the charged BBMB black hole but not for scalarized charged black holes.

## 2 EMCS theory and its black holes

We start with the Einstein-Maxwell-conformally coupled scalar (EMCS) theory given by

$$S_{\text{EMCS}} = \frac{1}{16\pi G} \int d^4x \sqrt{-g} \left[ R - F_{\mu\nu} F^{\mu\nu} - \beta \left( \phi^2 R + 6\partial_\mu \phi \partial^\mu \phi \right) \right], \quad (1)$$

where the last term corresponds to a conformally coupled scalar action with parameter  $\beta$ . This action has no Weyl symmetry (under Weyl rescaling:  $g_{\mu\nu} \rightarrow \Omega^2 g_{\mu\nu}$ ,  $\phi \rightarrow \phi/\Omega$ ,  $F_{\mu\nu} \rightarrow F_{\mu\nu}$ ) because the Ricci scalar  $R$  is present. In the absence of Maxwell term, it corresponds to the Einstein-conformally coupled scalar theory which provides the BBMB black hole solution. From Eq.(1), Bekenstein has obtained the charged BBMB black hole solution [4] and then, Astorino has found the constant scalar hairy black hole solution [21]. In this work, we choose  $\beta = \kappa/6 = 4\pi G/3$ .

Einstein equation is derived from Eq.(1) as

$$G_{\mu\nu} = 2T_{\mu\nu}^{\text{M}} + T_{\mu\nu}^{\phi} \quad (2)$$

with the Einstein tensor is given by  $G_{\mu\nu} = R_{\mu\nu} - Rg_{\mu\nu}/2$ . Here, two energy-momentum tensors for Maxwell theory and conformally coupled scalar theory are defined by

$$\begin{aligned} T_{\mu\nu}^{\text{M}} &= F_{\mu\rho} F_{\nu}{}^{\rho} - \frac{F^2}{4} g_{\mu\nu}, \\ T_{\mu\nu}^{\phi} &= \beta \left[ \phi^2 G_{\mu\nu} + g_{\mu\nu} \nabla^2(\phi^2) - \nabla_\mu \nabla_\nu(\phi^2) + 6\nabla_\mu \phi \nabla_\nu \phi - 3(\nabla\phi)^2 g_{\mu\nu} \right]. \end{aligned} \quad (3)$$

At this stage, we check the traceless condition of  $T_{\mu}^{\text{M},\mu} = 0$  easily. The Maxwell equation takes the form

$$\nabla^\mu F_{\mu\nu} = 0. \quad (4)$$

Lastly, the scalar equation is given by

$$\nabla^2\phi - \frac{1}{6}R\phi = 0. \quad (5)$$

Even though  $T_\mu^{\phi,\mu} = \beta\phi(-R\phi + 6\nabla^2\phi)$  is not zero apparently, making use of the scalar equation (5) leads to a traceless case of  $T_\mu^{\phi,\mu} = 0$ . This implies that  $T_\mu^{\phi,\mu}$  vanishes on-shell configurations. On the other hand, taking the trace of the Einstein equation (2) together with (5) leads to a vanishing Ricci scalar as

$$R = 0. \quad (6)$$

Plugging this back into Eq.(5) simplifies it as

$$\nabla^2\phi = 0. \quad (7)$$

One finds the constant scalar hairy (charged) black hole solution given by [21]

$$\begin{aligned} ds_{\text{cshbh}}^2 &= \bar{g}_{\mu\nu}dx^\mu dx^\nu = -N(r)dt^2 + \frac{dr^2}{N(r)} + r^2d\Omega_2^2, \\ N(r) &= 1 - \frac{2m}{r} + \frac{Q^2 + S}{r^2}, \\ \bar{\phi}_\pm &= \pm\sqrt{\frac{1}{\beta}}\sqrt{\frac{S}{Q^2 + S}}, \quad \bar{A}_t = \frac{Q}{r} - \frac{Q}{r_+}. \end{aligned} \quad (8)$$

This is derived mainly from solving the background Einstein equation

$$\bar{R}_{\mu\nu} = \frac{2\bar{T}_{\mu\nu}^M}{1 - \beta\bar{\phi}^2} \equiv 2\bar{T}_{\mu\nu} \quad (9)$$

with the traceless energy-momentum tensor

$$\bar{T}^\mu{}_\nu = \frac{Q^2 + S}{r^4} \text{diag}[-1, -1, 1, 1]. \quad (10)$$

Considering an anisotropic matter with  $T^\mu{}_\nu = \text{diag}[-\rho, p, p_T, p_T]$ , we have corresponding energy density and pressures

$$\rho = p_T = \frac{Q^2 + S}{r^4}, \quad p = -\frac{Q^2 + S}{r^4}. \quad (11)$$

Imposing  $N(r) = 0$ , the locations of outer and inner horizons are determined by

$$r_\pm = m \pm \sqrt{m^2 - Q^2 - S}. \quad (12)$$

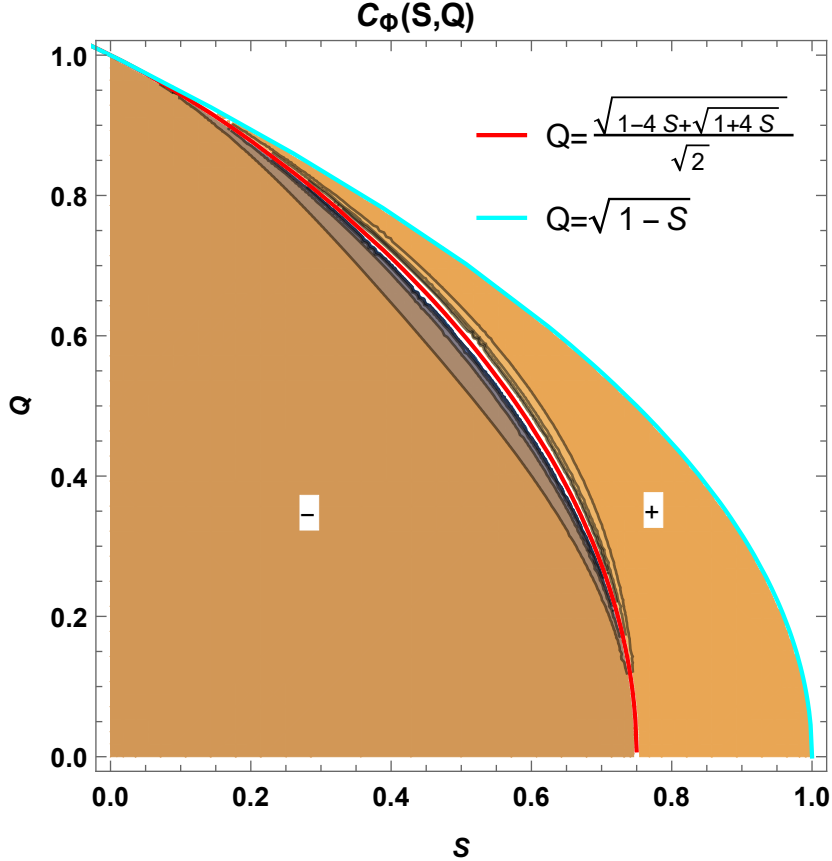


Figure 1: Contour plot of heat capacity  $C_\Phi$  for SHRN black holes as function of scalar hair  $S \in [0, 1]$  and electric charge  $Q \in [0, 1]$ . A red curve  $Q = \sqrt{1-4S} + \sqrt{1+4S}/\sqrt{2}$  represents a boundary (Davies curve:  $C_\Phi \rightarrow \infty$ ) between negative region (-: unstable) and positive region (+: stable). A cyan curve  $Q = \sqrt{1-S}$  denotes a boundary ( $C_\Phi = 0$ ) between SHRN black holes and naked singularity.

This black hole seems to have a primary scalar hair and its geometry is similar to a non-extremal RN black hole except that the position of the horizon is shifted by the presence of the scalar charge  $S$ . However, we wish to mention that a constant scalar  $\bar{\phi}_+ (> 0)$  depends on both  $S$  and  $Q$ , implying that it is not strictly a primary hair. We note here that the case of  $Q = \sqrt{-S}$  denotes Schwarzschild-like black hole (Schwarzschild black hole with  $S = Q = 0$ ) and the case of  $Q = \sqrt{m^2 - S}$  represents extremal black hole (extremal RN black hole with  $S = 0$ ). We point out from Eq.(10) that the background energy-momentum tensor  $\bar{T}^\mu{}_\nu$  is always traceless, and it satisfies both dominant and strong energy conditions

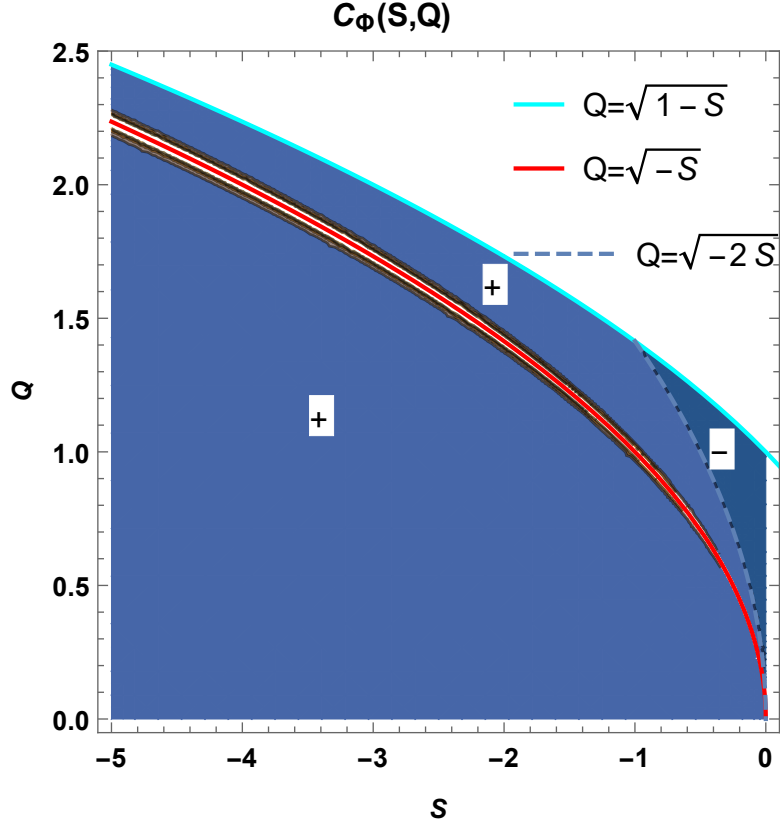


Figure 2: Contour plot of heat capacity  $C_\Phi$  for scalar hairy charged and mutated-RN black holes as function of scalar hair  $S \in [-5, 0]$  and electric charge  $Q \in [0, 2.5]$ . A red curve  $Q = \sqrt{-S}$  represents a boundary (Davies curve:  $C_\Phi \rightarrow \infty$ ) between positive (+) region (mutated RN black holes) and positive (+) region (scalar hairy charged black holes). A cyan curve  $Q = \sqrt{1-S}$  denotes a boundary ( $C_\Phi = 0$ ) between scalar hairy charged black holes and naked singularity, while a dashed line  $Q = \sqrt{-2S}$  represents a boundary ( $C_\Phi = 0$ ) between positive region (+: stable) and negative region (-: unstable) in scalar hairy charged black holes.

whenever  $S \geq -Q^2$  [21]. This implies that two energy conditions violate for  $S < -Q^2$ . Also, we observe from Eq.(9) that for  $1 - \beta\bar{\phi}_+^2 \neq 0$  ( $Q \neq 0$ ), the presence of a constant conformally coupled scalar field rescales the Newton constant  $G$  as  $\tilde{G} = G/(1 - \beta\bar{\phi}_+^2) = G(Q^2 + S)/Q^2$ . This effective Newton constant should be positive. This is possible whenever  $S > -Q^2$  that corresponds to the condition for respecting both dominant and strong energy conditions. For  $S = -Q^2$ , one finds an unwanted case of  $\tilde{G} = 0$ .

Furthermore, its thermodynamic quantities are well established when replacing the Newton constant  $G$  with the effective Newton constant  $\tilde{G} \neq 0$ : ADM mass  $M = \frac{m}{\tilde{G}}$  and entropy  $S = \frac{A_+}{4\tilde{G}}$ . We stress that two quantities are always positive for  $\tilde{G} > 0 (S > -Q^2)$ . The ADM mass and entropy go to zero when the electric charge  $Q$  approaches zero. This suggests that the constant scalar hairy charged black hole cannot radiate away its charge  $Q$  and settle down to a constant scalar hairy (uncharged) black hole. The local thermodynamic stability can be determined by the heat capacity at constant electric potential  $C_\Phi$  and the electric permittivity at constant temperature  $\epsilon_T$  in the grand canonical ensemble defined by

$$C_\Phi = T \left( \frac{\partial S}{\partial T} \right)_\Phi = - \frac{2\pi r_+ Q^2 (Q^2 + 2S)(r_+^2 - Q^2 - S)}{(Q^2 + S)^2 (r_+^2 - Q^2 - 3S)}, \quad (13)$$

$$\epsilon_T = \left( \frac{\partial Q}{\partial \Phi} \right)_T = \frac{r_+ (r_+^2 - 3Q^2 - 3S)}{r_+^2 - Q^2 - 3S}, \quad (14)$$

where the Hawking temperature is well-defined by

$$T = \frac{r_+ - r_-}{4\pi r_+^2} \geq 0. \quad (15)$$

The zero temperature is for an extremal black hole with  $Q = \sqrt{1 - S}$ . In this case, we confirm that the first-law of thermodynamics for black hole is satisfied.  $C_\Phi$  blows up at  $Q = \sqrt{-S}$ ,  $\sqrt{1 - 4S + \sqrt{1 + 4S}}/\sqrt{2}$  and it vanishes at  $Q = \sqrt{1 - S}$ ,  $\sqrt{-2S}$ . Its sign-dependence is shown in Fig. 1 for  $0 < S < 1$  and Fig. 2 for  $-5 < S < 0$ . A positive region (+:  $C_\Phi > 0$ ) represents a thermodynamically stable region, a negative region ( $-$ :  $C_\Phi < 0$ ) represents a thermodynamically unstable region, and a red curve denotes Davies curve ( $C_\Phi \rightarrow \infty$ ). On the other hand,  $\epsilon_T$  blows up at  $Q = \sqrt{1 - 4S + \sqrt{1 + 4S}}/\sqrt{2}$  and it is zero at  $Q = \sqrt{3 - 4S}/2$ ,  $\sqrt{1 - S}$ . We note that it is positive mostly but negative for narrow strips as  $\sqrt{3 - 4S}/2 < Q < \sqrt{1 - 4S + \sqrt{1 + 4S}}/\sqrt{2}$  ( $0 < S < 1$ ) and  $\sqrt{3 - 4S}/2 < Q < \sqrt{1 - S}$  ( $-5 < S < 0$ ). Thus, we do not display it and we will not mention  $\epsilon_T$  for discussion of real bounds.

For our purpose, we classify constant scalar hairy charged black holes with  $m = 1$  into three cases: scalar hairy RN (SHRN) black holes with  $0 < S < 1$  and  $0 < Q < \sqrt{1 - S}$ , scalar hairy charged black hole with  $-Q^2 < S < 0$ , and mutated-RN black hole (Einstein-Rosen bridge) with  $S < -Q^2$ . In addition, the case of  $Q = \sqrt{-S}$  represents a boundary curve (Schwarzschild-like black hole) where the scalar  $\bar{\phi}_+$  blows up. It is important to note that the case of  $Q = \sqrt{1 - S}$  denotes the outer boundary (extremal black hole) between

scalar hairy black holes and naked singularity. It is worth noting that SHRN black holes with  $0 < S < 1$  and  $0 < Q < \sqrt{1 - S}$  are stable against full perturbations [25].

### 3 Photon ring bounds

Recently, it was found that the lower bound on the photon ring radius  $r_\gamma$  of black holes found in Einstein gravity with a traceless energy-momentum tensor  $T^\mu{}_\nu = \text{diag}[-\rho, p, p_T, p_T]$  and  $\rho(\geq 0) \geq |p|, |p_T|$  is given by [15]

$$r_\gamma \geq 1.2r_+. \quad (16)$$

Two known examples to be tested are RN and Einstein-Yang-Mills black holes. In the case of RN black hole, one finds that  $r_\gamma/r_+ = 1.5$  for  $Q = 0$  (Schwarzschild black hole) and  $r_\gamma/r_+ = 2$  for  $Q = M$  (extremal RN Black hole). Its real bound is given by  $1.5 \leq r_\gamma/r_+ \leq 2$ . However, it is not easy to test Einstein-Yang-Mills black holes because their solutions were known numerically [16, 17, 18, 19, 20], even though Hod has focussed on this black hole.

Here, we wish to derive the ratio of  $r_\gamma/r_+$  to obtain the real bounds of photon rings for constant scalar hairy charged black holes because the background energy-momentum tensor  $\bar{T}^\mu{}_\nu$ , Eq.(10) is always traceless. For this purpose, the effective potential for null geodesics is given by [26]

$$V(r) = \frac{\sqrt{N(r)}}{r}. \quad (17)$$

A photon ring corresponds to a critical point of  $V(r)$ , that is,

$$V'(r)|_{r=r_\gamma} = 0. \quad (18)$$

In this case, one finds a photon ring radius with  $m = 1$  as

$$r_\gamma = \frac{3}{2} \left[ 1 + \sqrt{1 - \frac{8}{9}(S + Q^2)} \right]. \quad (19)$$

The ratio of  $r_\gamma$  to  $r_+$  is defined as

$$\frac{r_\gamma}{r_+} = \frac{\frac{3}{2} \left[ 1 + \sqrt{1 - \frac{8}{9}(Q^2 + S)} \right]}{1 + \sqrt{1 - (Q^2 + S)}}. \quad (20)$$

We find interesting three ratios from Fig. 3: 1.5 (Schwarzschild black hole) for  $Q = \sqrt{-S}$ , 2 (extremal RN black hole) for  $Q = \sqrt{1 - S}$ , and 1.45 at a point of  $(S = -5, Q = 0)$ . Also, one obtains  $\frac{r_\gamma}{r_+} = \sqrt{2} = 1.414$  for  $S = -\infty$ , irrespective of  $Q$ .

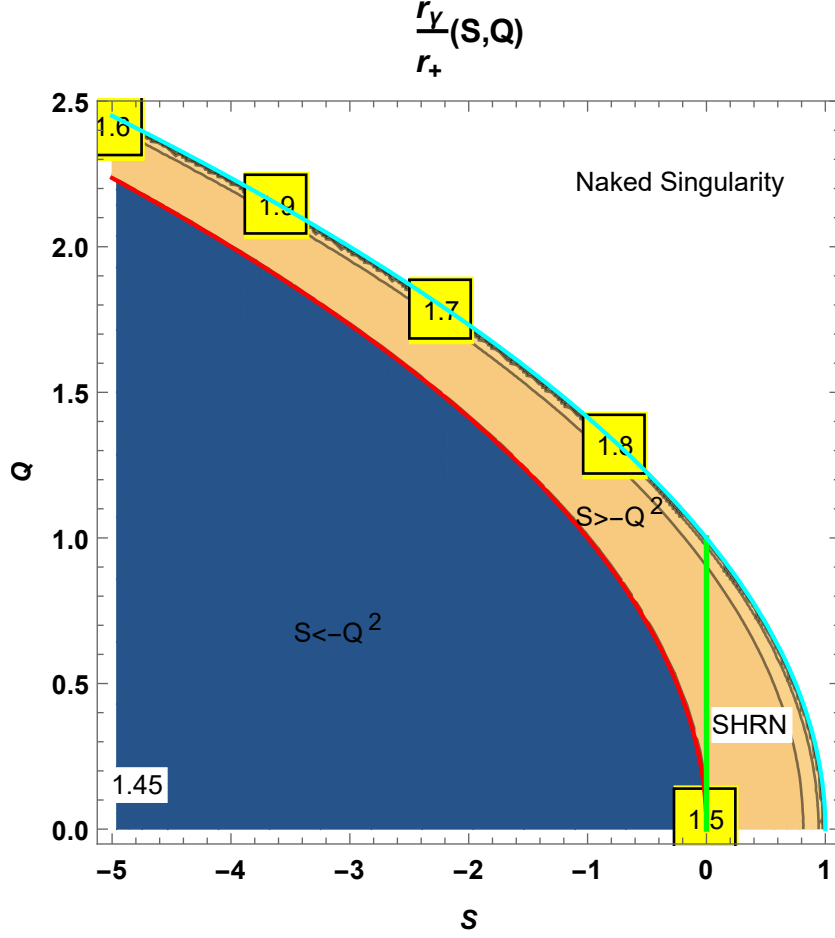


Figure 3: Contour plot of  $\frac{r_\gamma}{r_+}$  as function of scalar hair  $S \in [1, -5]$  and electric charge  $Q \in [0, 2.5]$ . A red curve  $Q = \sqrt{-S}$  represents a boundary (Schwarzschild-like black hole with  $\frac{r_\gamma}{r_+} = 1.5$ ) between scalar hairy charged black hole with  $-Q^2 < S < 0$  and mutated-RN black hole with  $S < -Q^2$ . A cyan curve  $Q = \sqrt{1-S}$  denotes a boundary (extremal black hole with  $\frac{r_\gamma}{r_+} = 2$ ) between black holes with  $-Q^2 < S < 0$  and naked singularity with  $S > 1 - Q^2$ . The right of a green line represents the SHRN black holes with  $0 < S < 1$  and  $0 < Q < \sqrt{1-S}$ . At a point of  $(S = -5, Q = 0)$ , one finds the lowest ratio of  $\frac{r_\gamma}{r_+} = 1.45$ .

We wish to classify all bounds according to the ratio.

1)  $1.2 \leq r_\gamma/r_+ < 1.414$

We could not find any constant scalar hairy charged black holes, belonging to this bound.

2)  $1.414 \leq r_\gamma/r_+ < 1.5$

Mutated-RN black holes (Einstein-Rosen bridge: wormhole) with  $S < -Q^2$  belong to this

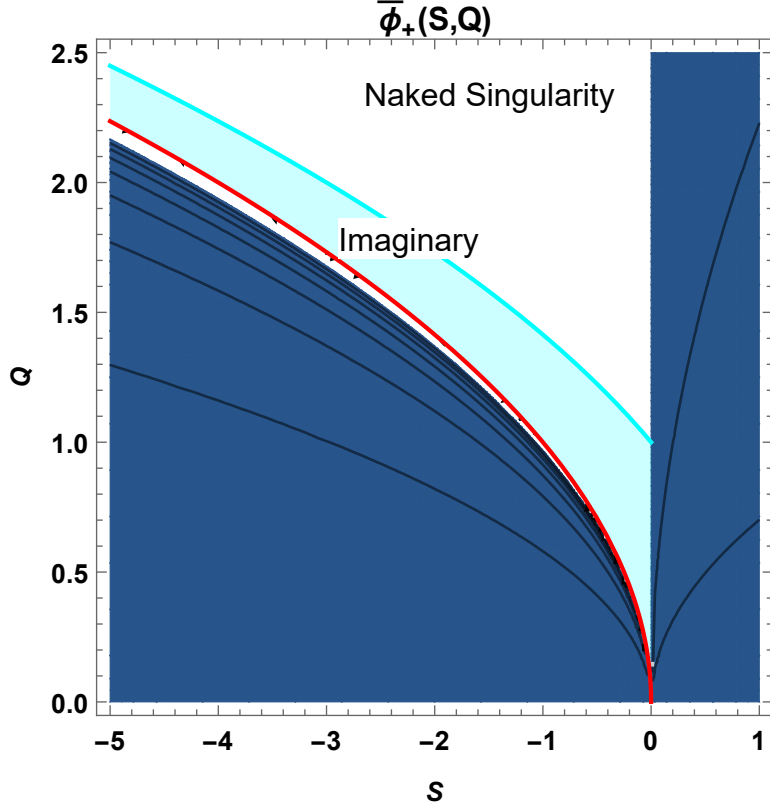


Figure 4: Contour plot of scalar  $\bar{\phi}_+$  as function of scalar hair  $S \in [-5, 1]$  and electric charge  $Q \in [0, 2.5]$ . A red curve  $Q = \sqrt{-S}$  represents a boundary (Schwarzschild-like black hole) with an infinite scalar. A cyan curve  $Q = \sqrt{1-S}$  denotes a boundary (extremal black hole) between scalar hairy black holes with  $-Q^2 < S < 0$  and naked singularity with  $S > 1 - Q^2$ . The scalar is imaginary between red and cyan curves for  $S < 0$ . The shaded region represents real scalar.

category. All of these black holes are unsatisfied with dominant and strong energy conditions, even though their scalar is real (see Fig. 4). Also, we mention that all mutated-RN black holes do not possess positive ADM mass and entropy, and are thermodynamically stable (+) (see Fig. 2). However, we wish to point out that this bound was included to set a rough limit for the shadow of M87\* within  $1\sigma(-1.5 \lesssim S \lesssim 0$ : thermodynamically stable region) [22].

$$3) r_\gamma/r_+ = 1.5(Q = \sqrt{-S})$$

Schwarzschild-like black hole provides this ratio exactly with an infinite scalar (see Fig. 4).

This represents Davies curve where the heat capacity blows up.

4)  $1.5 < r_\gamma/r_+ < 2.0(S > 0)$

All SHRN black holes with  $0 < S < 1$  and  $0 < Q < \sqrt{1-S}$  satisfy this bound. Their scalar is always real (see Fig. 4). The region of  $Q < \sqrt{1-4S + \sqrt{1+4S}}/\sqrt{2}$  is thermodynamically unstable, while other region of  $Q > \sqrt{1-4S + \sqrt{1+4S}}/\sqrt{2}$  is thermodynamically stable (see Fig. 1). These black holes respect both dominant and strong energy conditions and have positive ADM mass and entropy. These black holes are stable against full perturbations. Importantly, this bound includes the shadow of M87\* within  $1\sigma$  [22]. In this case, the EHT [13] sets a rough upper bound of  $S \leq 0.4$  for  $Q \ll 1$  (thermodynamically unstable region).

5)  $1.5 < r_\gamma/r_+ < 2.0(S < 0)$

This bound holds for all constant scalar hairy charged black holes with  $-Q^2 < S < 0$ . These black holes respect both dominant and strong energy conditions, and have positive ADM mass and entropy. There are two regions: thermodynamically stable region ( $Q < \sqrt{-2S}$ ) is bigger than thermodynamically unstable region ( $Q > \sqrt{-2S}$ ) (see Fig. 2). Unfortunately, the scalar  $\bar{\phi}_+$  is imaginary (see Fig. 4). So, this bound was discarded for testing the shadow of M87\* [22] and gravitational lensing effects [23]. However, these black holes seem to be better physically than mutated-RN black holes.

6)  $r_\gamma/r_+ = 2.0(Q = \sqrt{1-S})$

The extremal black holes belong to this case. Their temperature and heat capacity vanish.

7)  $r_\gamma/r_+ > 2.0$

No such constant scalar hairy black holes are found within this lower bound.

Consequently, all constant scalar hairy charged black holes respect the lower bound (16) for photon rings.

Finally, we mention two other black hole solutions obtained from the EMCS theory: charged BBMB and scalarized charged black holes. The charged BBMB black hole is given by [4]

$$ds_{\text{cBBMP}}^2 = -\left(1 - \frac{m}{r}\right)^2 dt^2 + \frac{dr^2}{\left(1 - \frac{m}{r}\right)^2} + r^2 d\Omega_2^2,$$

$$\bar{\phi}_{B\pm}(r) = \pm \sqrt{\frac{1}{\beta}} \frac{S}{r - m}, \quad \bar{A}_t = \frac{Q}{r} - \frac{Q}{r_+}, \quad m = \sqrt{Q^2 + S^2}, \quad (21)$$

where  $m(Q, S)$  is the mass (electric charge, scalar hair) of the black hole. Here, the scalar

$\bar{\phi}_B(r)$  is the solution to  $\bar{\nabla}^2 \bar{\phi} = 0 \rightarrow 2\bar{\phi}'^2 - \bar{\phi}''\bar{\phi} = 0$ . This line element takes the same form as in the extremal RN black hole, but the scalar blows up at the horizon  $r = m$  and it belongs to the secondary hair. The thermodynamical properties of the charged BBMB black hole are still bad because the Hawking temperature is always zero and the entropy becomes infinite. So, one argues that this might not be a physical black hole. Furthermore, it was shown that this black hole is unstable against the scalar perturbation [27] because it belongs to an extremal RN black hole [28]. Anyway, we can determine its ratio of photon ring radius to horizon radius as  $r_\gamma = 2m$  because it is an extremal black hole. Also, its effective Newton constant at photon ring [ $\tilde{G}|_{r=2m} = G/(1 - \beta\bar{\phi}_{B\pm}^2(r))|_{r=2m} = GQ^2/(Q^2 + S^2)$ ] takes a finite value, compared to  $\tilde{G}|_{r=2m} = G/(1 - \beta\bar{\phi}^2(r))|_{r=2m} \rightarrow \infty$  for the BBMB black hole [9].

One has obtained scalarized charged black holes numerically from the action of  $\dots [R - (1 + \alpha\phi^2) F_{\mu\nu}F^{\mu\nu} \dots]$  which includes a scalar coupling ( $\alpha\phi^2$ ) to Maxwell term in the EMCS theory (1) [25]. This scalar coupling is necessary to obtain single branch of scalarized charged black holes whose scalar differ from that for constant scalar hairy charged black holes in Eq.(8). In this case, we could not obtain the traceless energy-momentum tensor for scalar even on-shell configuration. So, we could not apply the lower bound Eq.(16) to these black holes. Consequently, we could not obtain an explicit form for the ratio of photon ring to horizon because scalarized charged black holes are found numerically as in Einstein-Yang-Mills black holes.

## 4 Discussions

We have revisited constant scalar hairy black holes with mass  $m$ , charge  $Q$ , and scalar hair  $S$  obtained from the Einstein-Maxwell-conformally coupled scalar theory. In this case, its background energy-momentum tensor Eq.(10) is always traceless. These black holes are composed of SHRN black hole, scalar hairy charged black hole with  $S \geq -Q^2$ , and mutated-RN black hole (Einstein-Rosen bridge). These black holes could be candidates for testing whether they satisfy the lower bound of photon ring of  $r_\gamma \geq 1.2r_+$  proposed in [15]. We have obtained all real bounds of photon rings for these black holes and discussed physical and observational properties of real bounds.

The first and second ones respect both dominant and strong energy conditions and, show positive ADM mass and entropy as well as positive effective Newton constant. We remind

the reader that the scalar of the first is real, while the scalar of the second is imaginary. The first (SHRN black hole) belongs to a good category to test observational properties of M87\* and SgrA\* supermassive black holes. The observational property prefers thermodynamically unstable region of  $Q < \sqrt{1 - 4S + \sqrt{1 + 4S}}/\sqrt{2}$  than thermodynamically stable region  $Q > \sqrt{1 - 4S + \sqrt{1 + 4S}}/\sqrt{2}$ . The second was discarded from the description for the shadow of M87\* supermassive black hole [22] and gravitational lensing effects of M87\* and SgrA\* supermassive black holes [23] because its scalar is imaginary. Here are two regions: thermodynamically stable ( $Q < \sqrt{-2S}$ ) and unstable regions ( $Q > \sqrt{-2S}$ ). We propose that the second should be included to test observational property of supermassive black holes.

On the other hand, the last (Einstein-Rosen bridge, wormholes) does not respect two energy conditions and show negative ADM mass and entropy as well as negative effective Newton constant. So, this case has some handicaps to be physical black holes. We note that the last is always thermodynamically stable (+). However, this (thermodynamically stable region) was included as the description for the shadow of M87\* supermassive black hole [22] and gravitational lensing effects of M87\* and SgrA\* supermassive black holes [23]. It seems promising that the last is not included to test observational property of supermassive black holes.

Consequently, all constant scalar hairy charged black holes respect the lower bound (16) for photon rings. At this stage, it is not clear that which thermodynamical region (+ or - heat capacity) is better to use for describing observational properties of supermassive black holes.

## References

- [1] R. Ruffini and J. A. Wheeler, *Phys. Today* **24**, no.1, 30 (1971) doi:10.1063/1.3022513
- [2] C. A. R. Herdeiro and E. Radu, *Int. J. Mod. Phys. D* **24**, no.09, 1542014 (2015) doi:10.1142/S0218271815420146 [arXiv:1504.08209 [gr-qc]].
- [3] N. M. Bocharova, K. A. Bronnikov and V. N. Melnikov, *Vestn. Mosk. Univ. Ser. III Fiz. Astron. ,* no. 6, 706 (1970).
- [4] J. D. Bekenstein, *Annals Phys.* **82**, 535-547 (1974) doi:10.1016/0003-4916(74)90124-9
- [5] E. Winstanley, *Conf. Proc. C* **0405132**, 305-323 (2004) [arXiv:gr-qc/0408046 [gr-qc]].
- [6] T. Karakasis, E. Papantonopoulos, Z. Y. Tang and B. Wang, *Eur. Phys. J. C* **81**, no.10, 897 (2021) doi:10.1140/epjc/s10052-021-09717-1 [arXiv:2103.14141 [gr-qc]].
- [7] T. Kobayashi, H. Motohashi and T. Suyama, *Phys. Rev. D* **89**, no.8, 084042 (2014) doi:10.1103/PhysRevD.89.084042 [arXiv:1402.6740 [gr-qc]].
- [8] Y. S. Myung and D. C. Zou, *Phys. Rev. D* **100**, no.6, 064057 (2019) doi:10.1103/PhysRevD.100.064057 [arXiv:1907.09676 [gr-qc]].
- [9] T. Shinohara, Y. Tomikawa, K. Izumi and T. Shiromizu, *PTEP* **2021**, no.9, 093E02 (2021) doi:10.1093/ptep/ptab107 [arXiv:2107.13133 [hep-th]].
- [10] Y. Tomikawa, T. Shiromizu and K. Izumi, *Class. Quant. Grav.* **34**, no.15, 155004 (2017) doi:10.1088/1361-6382/aa7906 [arXiv:1702.05682 [gr-qc]].
- [11] H. Yoshino, K. Izumi, T. Shiromizu and Y. Tomikawa, *PTEP* **2017**, no.6, 063E01 (2017) doi:10.1093/ptep/ptx072 [arXiv:1704.04637 [gr-qc]].
- [12] I. Z. Stefanov, S. S. Yazadjiev and G. G. Gylchev, *Phys. Rev. Lett.* **104**, 251103 (2010) doi:10.1103/PhysRevLett.104.251103 [arXiv:1003.1609 [gr-qc]].
- [13] K. Akiyama *et al.* [Event Horizon Telescope], *Astrophys. J. Lett.* **875**, L1 (2019) doi:10.3847/2041-8213/ab0ec7 [arXiv:1906.11238 [astro-ph.GA]].
- [14] P. V. P. Cunha and C. A. R. Herdeiro, *Phys. Rev. Lett.* **124**, no.18, 181101 (2020) doi:10.1103/PhysRevLett.124.181101 [arXiv:2003.06445 [gr-qc]].

- [15] S. Hod, *JHEP* **12**, 178 (2023) doi:10.1007/JHEP12(2023)178 [arXiv:2311.17462 [gr-qc]].
- [16] P. Bizon, *Phys. Rev. Lett.* **64**, 2844-2847 (1990) doi:10.1103/PhysRevLett.64.2844
- [17] E. Winstanley, *Class. Quant. Grav.* **16**, 1963-1978 (1999) doi:10.1088/0264-9381/16/6/325 [arXiv:gr-qc/9812064 [gr-qc]].
- [18] J. Bjoraker and Y. Hosotani, *Phys. Rev. D* **62**, 043513 (2000) doi:10.1103/PhysRevD.62.043513 [arXiv:hep-th/0002098 [hep-th]].
- [19] J. J. Van der Bij and E. Radu, *Phys. Lett. B* **536**, 107-113 (2002) doi:10.1016/S0370-2693(02)01808-7 [arXiv:gr-qc/0107065 [gr-qc]].
- [20] T. Moon, Y. S. Myung and E. J. Son, *Gen. Rel. Grav.* **43**, 3079-3098 (2011) doi:10.1007/s10714-011-1225-3 [arXiv:1101.1153 [gr-qc]].
- [21] M. Astorino, *Phys. Rev. D* **88**, no.10, 104027 (2013) doi:10.1103/PhysRevD.88.104027 [arXiv:1307.4021 [gr-qc]].
- [22] M. Khodadi, A. Allahyari, S. Vagnozzi and D. F. Mota, *JCAP* **09**, 026 (2020) doi:10.1088/1475-7516/2020/09/026 [arXiv:2005.05992 [gr-qc]].
- [23] Q. Qi, Y. Meng, X. J. Wang and X. M. Kuang, *Eur. Phys. J. C* **83**, no.11, 1043 (2023) doi:10.1140/epjc/s10052-023-12233-z
- [24] A. Chowdhury and N. Banerjee, *Eur. Phys. J. C* **78**, no.7, 594 (2018) doi:10.1140/epjc/s10052-018-6065-9 [arXiv:1807.09559 [gr-qc]].
- [25] D. C. Zou and Y. S. Myung, *Phys. Lett. B* **803**, 135332 (2020) doi:10.1016/j.physletb.2020.135332 [arXiv:1911.08062 [gr-qc]].
- [26] L. F. D. da Silva, F. S. N. Lobo, G. J. Olmo and D. Rubiera-Garcia, *Phys. Rev. D* **108**, no.8, 084055 (2023) doi:10.1103/PhysRevD.108.084055 [arXiv:2307.06778 [gr-qc]].
- [27] K. A. Bronnikov and Y. N. Kireev, *Phys. Lett. A* **67**, 95-96 (1978) doi:10.1016/0375-9601(78)90030-0
- [28] H. Onozawa, T. Mishima, T. Okamura and H. Ishihara, *Phys. Rev. D* **53**, 7033-7040 (1996) doi:10.1103/PhysRevD.53.7033 [arXiv:gr-qc/9603021 [gr-qc]].